

Analysis of *A4gnt* Knockout Mice Reveals an Essential Role for Gastric Sulfomucins in Preventing Gastritis Cystica Profunda

Masatomo Kawakubo, Hitomi Komura, Yukinobu Goso, Motohiro Okumura, Yoshiko Sato, Chifumi Fujii, Masaki Miyashita, Nobuhiko Arisaka, Satoru Harumiya, Kazuhiro Yamanoi, Shigenori Yamada, Shigeru Kakuta, Hiroto Kawashima, Michiko N. Fukuda, Minoru Fukuda, and Jun Nakayama*

Department of Molecular Pathology, Shinshu University School of Medicine (MK, HKo, MO, YS, CF, MM, NA, SH, KY, JN) and Institute for Biomedical Sciences, Interdisciplinary Cluster for Cutting Edge Research (MK, CF, KY, JN) and Research Center for Human and Environmental Sciences (SK), Shinshu University, Matsumoto, Japan; Department of Biochemistry, Kitasato University Graduate School of Medical Sciences, Sagami-hara, Japan (YG); Division of Gastroenterology, Iiyama Red Cross Hospital, Iiyama, Japan (SY); Department of Biomedical Science, Graduate School of Agricultural and Life Sciences, The University of Tokyo, Tokyo, Japan (SK); Laboratory of Microbiology and Immunology, Graduate School of Pharmaceutical Sciences, Chiba University, Chiba, Japan (HKa); Tumor Microenvironment and Cancer Immunology Program, Sanford Burnham Prebys Medical Discovery Institute, La Jolla, CA, USA (MNF, MF); and Laboratory for Drug Discovery, National Institute of Advanced Industrial Science and Technology, Tsukuba, Japan (MNF)

Summary

Gastric adenocarcinoma cells secrete sulfomucins, but their role in gastric tumorigenesis remains unclear. To address that question, we generated *A4gnt/Chst4* double-knockout (DKO) mice by crossing *A4gnt* knockout (KO) mice, which spontaneously develop gastric adenocarcinoma, with *Chst4* KO mice, which are deficient in the sulfotransferase GlcNAc6ST-2. *A4gnt/Chst4* DKO mice lack gastric sulfomucins but developed gastric adenocarcinoma. Unexpectedly, severe gastric erosion occurred in *A4gnt/Chst4* DKO mice at as early as 3 weeks of age, and with aging these lesions were accompanied by gastritis cystica profunda (GCP). *Cxcl1*, *Cxcl5*, *Ccl2*, and *Cxcr2* transcripts in gastric mucosa of 5-week-old *A4gnt/Chst4* DKO mice exhibiting both hyperplasia and severe erosion were significantly upregulated relative to age-matched *A4gnt* KO mice, which showed hyperplasia alone. However, upregulation of these genes disappeared in 50-week-old *A4gnt/Chst4* DKO mice exhibiting high-grade dysplasia/adenocarcinoma and GCP. Moreover, *Cxcl1* and *Cxcr2* were downregulated in *A4gnt/Chst4* DKO mice relative to age-matched *A4gnt* KO mice exhibiting adenocarcinoma alone. These combined results indicate that the presence of sulfomucins prevents severe gastric erosion followed by GCP in *A4gnt* KO mice by transiently regulating a set of inflammation-related genes, *Cxcl1*, *Cxcl5*, *Ccl2*, and *Cxcr2* at 5 weeks of age, although sulfomucins were not directly associated with gastric cancer development: (J Histochem Cytochem 67: 759–770, 2019)

Keywords

A4gnt, *Chst4*, double knockout mouse, gastritis cystica profunda, gastric mucin, O-glycan

Introduction

Sulfomucins are composed of sulfated O-glycans attached to specific scaffold proteins such as CD34 in humans and mice or GlyCAM1 in mice and play important roles in various physiological and pathological conditions.^{1–3} For example, involvement of sulfomucins in

Received for publication February 20, 2019; accepted June 6, 2019.

*Member of The Histochemical Society at the time of publication.

Corresponding Author:

Jun Nakayama, Department of Molecular Pathology, Shinshu University School of Medicine, Asahi 3-1-1, Matsumoto 390-8621, Japan.
E-mail: jnaka@shinshu-u.ac.jp

lymphocyte homing is well documented: O-glycans carrying 6-sulfo sialyl Lewis X recognize their specific receptor L-selectin expressed on high endothelial venules (HEV) in secondary lymphoid tissues such as lymph nodes⁴⁻⁷ or HEV-like vessels in chronic inflammatory sites such as chronic active gastritis associated with *Helicobacter pylori* infection⁸ and ulcerative colitis.⁹ Sulfomucins have long been recognized as produced by gastric adenocarcinoma cells.¹⁰ However, their role in gastric tumorigenesis has not been fully elucidated.

O-glycans containing terminal α 1,4-linked *N*-acetylglucosamine residues (α GlcNAc) are unique to the gland mucin secreted from pyloric gland cells and mucous neck cells of gastric mucosa and Brunner's gland cells of duodenal mucosa, and α 1,4-*N*-acetylglucosaminyltransferase (α 4GnT) is the sole enzyme that catalyzes α GlcNAc biosynthesis.¹¹ Previously, we generated knockout (KO) mice deficient in *A4gnt* which encodes α 4GnT, and showed that mutants spontaneously develop differentiated-type gastric adenocarcinoma accompanied by upregulation of the inflammation-related genes such as *Ccl2*, *Ili1*, and *Fgf7*, indicating tumor suppressor function of α GlcNAc in gastric cancer.¹² We also performed high iron diamin (HID) staining to detect sulfomucins¹³ in the gastric mucosa of *A4gnt* KO mice and observed abundant sulfomucin production in pyloric mucosa until 60-week-old of ages examined as opposed to minimal staining in wild type (WT) mice (personal communication [MK, JN]; also see supplemental Fig. S1). Sulfomucins contain sulfated residues, which are negatively charged. Thus, we hypothesized that sulfomucins secreted from gastric cancer cells attract inflammation-related, positively charged factors such as CCL2, interleukin (IL)-11, and FGF7, leading to progression of inflammation-related cancer.

To test this hypothesis, we decided to generate mutant mice lacking gastric sulfomucins on a background of *A4gnt* deficiency. To this end, we asked first which sulfotransferase(s) was responsible for sulfomucin biosynthesis in *A4gnt* KO mice. Mice harbor four sulfotransferase genes, including *Chst2*, *Chst4*, *Chst5*, and *Chst7*, which encode GlcNAc6ST-1, GlcNAc6ST-2, GlcNAc6ST-3, and GlcNAc6ST-4, respectively.² GlcNAc6ST-3 expression is limited to intestine and cornea. Therefore, we focused on comparing expression levels of *Chst2*, *Chst4*, and *Chst7* using RNA samples extracted from gastric mucosa of *A4gnt* KO or WT mice. We observed significant upregulation of *Chst4* in *A4gnt* KO relative to WT mice (supplemental Fig. S2), suggesting that sulfomucin overexpression in *A4gnt* KO mice is mediated by *Chst4* upregulation.

Therefore, here we generated *A4gnt/Chst4* double-knockout (DKO) mice. As expected, gastric sulfomucins were completely absent in mutant mice. However, contrary to expectations, *A4gnt/Chst4* DKO mice developed differentiated-type adenocarcinoma, indicating that sulfomucins play a minor role in gastric cancer progression. Surprisingly, prior to adenocarcinoma development, *A4gnt/Chst4* DKO mice exhibited unanticipated severe gastric erosion accompanied with aging by development of gastritis cystica profunda (GCP) beneath the erosion as seen in all 60-week-old *A4gnt/Chst4* DKO mice examined. These results provide unexpected evidence in a unique gastric cancer model *A4gnt* KO mouse that the presence of gastric sulfomucins maintains mucosal integrity and antagonizes development of GCP emerging from severe gastric erosion, which is seen in *A4gnt/Chst4* DKO mice.

Materials and Methods

Mice

Both *A4gnt* KO mice and *Chst4* KO mice were generated and maintained in autoclaved cages under specific pathogen-free conditions at the Animal Facility of Shinshu University, Matsumoto, Japan, as described.^{12,14} *A4gnt* KO mice were crossed with *Chst4* KO mice, and we obtained *A4gnt/Chst4* DKO, *A4gnt* KO mice, *Chst4* KO mice, and WT mice based on predicted Mendelian ratios (data not shown). Mice were genotyped using multiplex PCR analyses of *A4gnt* and *Chst4* alleles of tail DNA by using allele-specific primers: specifically, analysis using 3 primers (SAC-F [5'-ACG TGT GTC CTG ATA CCC TAG TGA-3'], SAW-R (5'-AGA TGA TGG GCT GCT CAG GAT AGA-3'), and SAN-R (5'-TCT CCT AGA GTT AAC ACT GGC CGT-3')) yielded 253-bp amplicons for *A4gnt* KO mice and 559-bp amplicons for WT mice, as described.¹² Another primer set (F2W [5'-AAG AAA GGG AGG CTG CTG ATG TTC-3'],¹⁴ R2W (5'-TCC ACC ATA TCA AAG GGC TGC TGA-3'),¹⁴ and EGFP-R3 (5'-AAG TCG TGC TGC TTC ATG TGG TCG-3')) yielded a 320-bp product in *Chst4* KO mice and a 478-bp product in WT mice. *A4gnt/Chst4* DKO mice or *Chst4* KO mice were bred until 60 weeks of age, and *A4gnt* KO mice and WT mice were bred until 50 weeks. The protocol for animal experiments was approved by the Animal Care Committee of Shinshu University and conducted in accordance with guidelines for use of laboratory animals at the same university (nos. 240057 and 280047).

Histopathology

A4gnt/Chst4 DKO and *Chst4* KO mice aged 3-weeks to 60-weeks as well as 3-week-old *A4gnt* KO and WT

mice were killed by cervical dislocation at the time points of 3-, 5-, 10-, 20-, 30-, 40-, 50-, and 60-weeks of age, and stomachs were removed with duodenum (n = 6 in each group). Stomachs were opened along the greater curvature, flattened by pinning, and fixed in 20% buffered formalin for 48 hr at 4°C. Each stomach was cut longitudinally into 5 pieces of equal width and embedded in paraffin. Serial 3- μ m sections were prepared from tissue blocks and subjected to H&E staining, mucin histochemistry, and immunohistochemistry, as described below. As needed, formalin-fixed and paraffin-embedded blocks of stomach tissue from *A4gnt* KO or WT mice aged 5 to 60 weeks were prepared, as described previously,¹² and reused based on the principle of the 3Rs (Replacement, Reduction and Refinement) in animal experiments.¹⁵ Gastric mucosal thickness was analyzed at a well-oriented representative pyloric gland using images of H&E-stained sections. Histopathology of gastric mucosa from *A4gnt/Chst4* DKO mice was classified into five categories, including normal mucosa, hyperplasia, low-grade dysplasia, high-grade dysplasia, and adenocarcinoma, based on criteria previously reported based on World Health Organization classification.¹⁶

Mucin Histochemistry and Immunohistochemistry

AB-PAS and HID-AB stainings were carried out on mouse gastric mucosa, as described.^{13,17} AB-PAS staining differentiated acidic mucins as blue-to-purple from neutral mucins as red, while HID-AB staining differentiated sulfomucins as black from sialomucins as light blue. For immunohistochemistry, α GlcNAc, Ki-67 antigen, and Ly-6G/Ly-6C (Gr-1) antigen were detected with primary antibodies HIK1083 (Kantokagaku, Tokyo, Japan), B56 (BD Biosciences, San Jose, CA), and RB6-8C5 (Biolegend, San Diego, CA), respectively.¹⁸⁻²⁰ Antigen retrieval for Ki-67 antigen was carried out by microwaving tissue slides in 10 mM Tris-HCl buffer (pH 8.0) plus 1 mM EDTA for 30 min. For Ly-6G/Ly-6C (Gr-1) antigen, tissue slides were digested with 0.25% Difco trypsin 250 (BD Biosciences, San Jose, CA) at 37°C for 30 min. As secondary antibodies, a Histofine Mousestain Kit (Nichirei Biosciences, Tokyo, Japan) was used for α GlcNAc and Ki-67 antigen, and a Histofine Simple Stain Mouse, MAX-PO (Rat) (Nichirei Biosciences) was used for Ly-6G/Ly-6C (Gr-1) antigen. Counterstaining was carried out using hematoxylin. Control immunohistochemistry was performed by omitting the primary antibody from the procedure, and no specific staining was seen (data not shown). The Ki-67 labeling index (LI) in mouse gastric

mucosa was determined by comparing the number of Ki-67-positive epithelial cells to the total number of epithelial cells in well-oriented pyloric glands in each mouse.

Oligosaccharide Analysis of Gastric O-glycans

Mice were killed as above, and glandular stomachs were removed with duodenum. Gastric mucins were extracted from the gastric mucosa of 10-week-old WT, *A4gnt* KO, and *A4gnt/Chst4* DKO mice (2 mice each) and purified by Sepharose CL-6B chromatography followed by CsTFA equilibrium centrifugation, as described.¹² Oligosaccharides were obtained by alkaline-borohydride treatment of mouse gastric mucins, as described,¹² except that neutral and acidic oligosaccharides were separated on a column (1.27 cm I.D. x 1.6 cm) of QAE-Toyopearl (acetate form, Tosoh, Tokyo, Japan). After applying oligosaccharides to the column, neutral oligosaccharides were washed from the column with water and acidic oligosaccharides were eluted with 0.4 M pyridinium acetate, pH 5. Oligosaccharides were then permethylated using the methods of Ciucanu and Costello.²¹ Acidic oligosaccharides were converted to triethylamine salt before permethylation, and permethylated oligosaccharides were recovered on an OASIS HLB column (30 mg/cc; Waters, Milford, MA), as described.²² Then, matrix-assisted laser desorption/ionization time-of-flight mass spectrometry (MALDI-TOF-MS) analysis of oligosaccharides was carried out. MALDI-TOF-MS spectra were acquired on a autoflex III mass spectrometer (Bruker Daltonics, Billerica, MA) equipped with a LIFT-MS/MS mode, using the following conditions: 2,5-dihydro benzoic acid served as the matrix, the positive ion mode was used, and all spectra were measured in the reflectron mode. A portion of the matrix solution (1 μ l) was applied to a stainless steel target, to which was added a solution (1 μ l) of oligosaccharides. The target was dried at ambient temperature for several minutes. Lacto-*N*-fucopentaose I, angiotensin and ACTH (1–24) were used for mass calibration. Fragment ion analysis by tandem mass spectrometry after laser-induced dissociation was performed according to the manufacturer's (Bruker Daltonics) operation manual. Data analyses were performed using GlycoWorkbench.²³

Quantitative RT-PCR

Mice were killed, and stomachs plus duodenum were removed as above. Fresh samples of glandular stomachs were extracted from *A4gnt/Chst4* DKO, *Chst4* KO, *A4gnt* KO, and WT mice at 5-, 10-, and 50-weeks

of age (4–6 mice each). Briefly, mucosa (~280 mg each) scraped off with a glass slide was transferred to a sterile 1.5 ml tube containing RNA later (Invitrogen, Carlsbad, CA). Gastric mucosa of 20 mg was used for extraction of total RNA using an RNeasy Mini Kit (Qiagen, Hilden, Germany), according to the manufacturer's protocol. RNA solution of 11 μl was combined with 0.5 μl of 0.5 mg/ml random primers (Promega, Madison, WI), 0.5 μl of 0.5 mg/ml oligo-dT primers (Promega), and 1 μl of a 2.5 mM dNTP mixture, denatured at 65°C for 5 min, and placed on ice. For single-stranded cDNA synthesis, samples were incubated with 1 μl of 200 U/ml SuperScript III (Invitrogen), 1 μl of 0.1 M dithiothreitol, 1 μl of 40 U/ml RNasin Plus RNase inhibitor (Promega), and 4 μl of 5 \times Fast Strand buffer (Invitrogen) at 50°C for 1 hr and then heated to 85°C for 5 min to terminate the reaction. Quantitative RT-PCR was performed using the 7300 Real-Time PCR System (Applied Biosystems, Foster City, CA). Premixed reagents containing primers and TaqMan probes for selected genes including *Cxcl1* (Assay ID: Mm00433851_ml), *Cxcl5* (Mm00436451_gl), *Cxcr2* (Mm99999117_sl), *Ccl2* (Mm00441242_ml), *Ccr2* (Mm99999051_gH), *Hgf* (Mm01135193_ml), *Met* (Mm01156972_ml), *Fgf7* (Mm00433291_ml), *Fgfr2b* (Mm01269930_ml), *Il1b* (Mm013336189_ml), *Il1r1* (Mm00434237_ml), *Il1r2* (Mm00439629_ml), *Il11* (Mm00434162_ml), *Il11ra1* (Mm01223545_ml), and *Gapdh* (Mm99999915_gl) were purchased from Applied Biosystems.

Statistics

Statistical analysis was carried out using ystat2013 software (Igaku Tosho Shuppan, Tokyo, Japan). Significance was evaluated by Student–Newman–Keuls test. All statistical data are presented as means \pm SEM, and a value of $P < 0.05$ was considered significant.

Results

Pyloric Gland Cells of A4gnt KO Mice Overproduce Sulfomucins

Using HID-AB staining, we detected sulfomucins (colored black by HID-AB staining) in pyloric gland cells of stomach in WT and *A4gnt* KO mice but not *Chst4* KO mice (Fig. 1A, HID-AB). However, based on HID-AB staining (compare WT versus *A4gnt* KO in Fig. 1A, pyloric mucosa panels), sulfomucin expression levels in pyloric gland cells that lacked αGlcNAc in *A4gnt* KO mice were clearly higher relative to pyloric gland cells positive for αGlcNAc in WT mice

(compare HID-AB versus HIK1083 in Fig. 1A, pyloric mucosa panels). On the other hand, goblet cells of duodenal mucosa in WT, *A4gnt* KO, and *Chst4* KO mice showed comparable sulfomucin levels (arrows in Fig. 1A, duodenal mucosa panels). By contrast, sulfomucin levels in mucous neck cells of fundic mucosa and Brunner's glands of the duodenum were minimal in WT and *A4gnt* KO mice and negative in *Chst4* KO mice (Fig. 1A, HID-AB, panels for fundic mucosa and duodenal mucosa). Neutral mucins (colored red by AB-PAS staining) were detected in Brunner's glands of WT mice and *Chst4* KO mice, while sialomucins (colored sky blue by HID-AB staining) were detected in Brunner's glands of *A4gnt* KO mice (Fig. 1A, AB-PAS and HID-AB, duodenal mucosa panels).

We then confirmed sulfomucin overproduction in pyloric gland cells of *A4gnt* KO mice by mass spectrometry using oligosaccharides prepared from mouse gastric mucosa (Fig. 1B). Analysis of the acidic oligosaccharide fraction revealed three species of sulfated O-glycans—Fuc-Gal-(SO₃-GlcNAc-)GalNAc, Fuc-Gal-(Fuc-Gal-[SO₃-]GlcNAc-)GalNAc, and Fuc-Gal-(Neu5Ac-Gal-(SO₃-)GlcNAc-)GalNAc—in *A4gnt* KO but not WT mice. However, as reported previously¹² and confirmed here, analysis of neutral oligosaccharides showed seven peaks indicative of αGlcNAc -containing O-glycans in WT mice, but those peaks were completely absent in *A4gnt* KO mice.

A4gnt/Chst4 DKO Mice Lack Gastric Sulfomucins

Next, we generated *A4gnt/Chst4* DKO mice to assess function of gastric sulfomucins. *A4gnt/Chst4* DKO mice developed to adulthood and reproduced normally (data not shown). Immunostaining with HIK1083 antibody revealed complete lack of αGlcNAc in gastroduodenal mucosa of *A4gnt/Chst4* DKO mice (Fig. 1A, HIK1083). In addition, HID-AB staining of pyloric gland cells from *A4gnt/Chst4* DKO mice revealed complete loss of sulfomucins in pyloric gland cells, while these mucous cells were positive for sialomucins (Fig. 1A, light blue by HID-AB staining). On the other hand, sulfomucins remained in duodenal goblet cells of *A4gnt/Chst4* DKO mice at levels comparable to those seen in WT and *A4gnt* KO mice (arrows in Fig. 1A, HID-AB). Sialomucins were detected in Brunner's glands of duodenal mucosa in *A4gnt/Chst4* DKO mice like *A4gnt* KO mice. However, sulfomucins were not detectable in Brunner's glands in *A4gnt/Chst4* DKO mice.

We next confirmed sulfomucin loss in *A4gnt/Chst4* DKO mice by mass spectrometry (Fig. 1B). Following acidic oligosaccharide analysis, it was revealed that

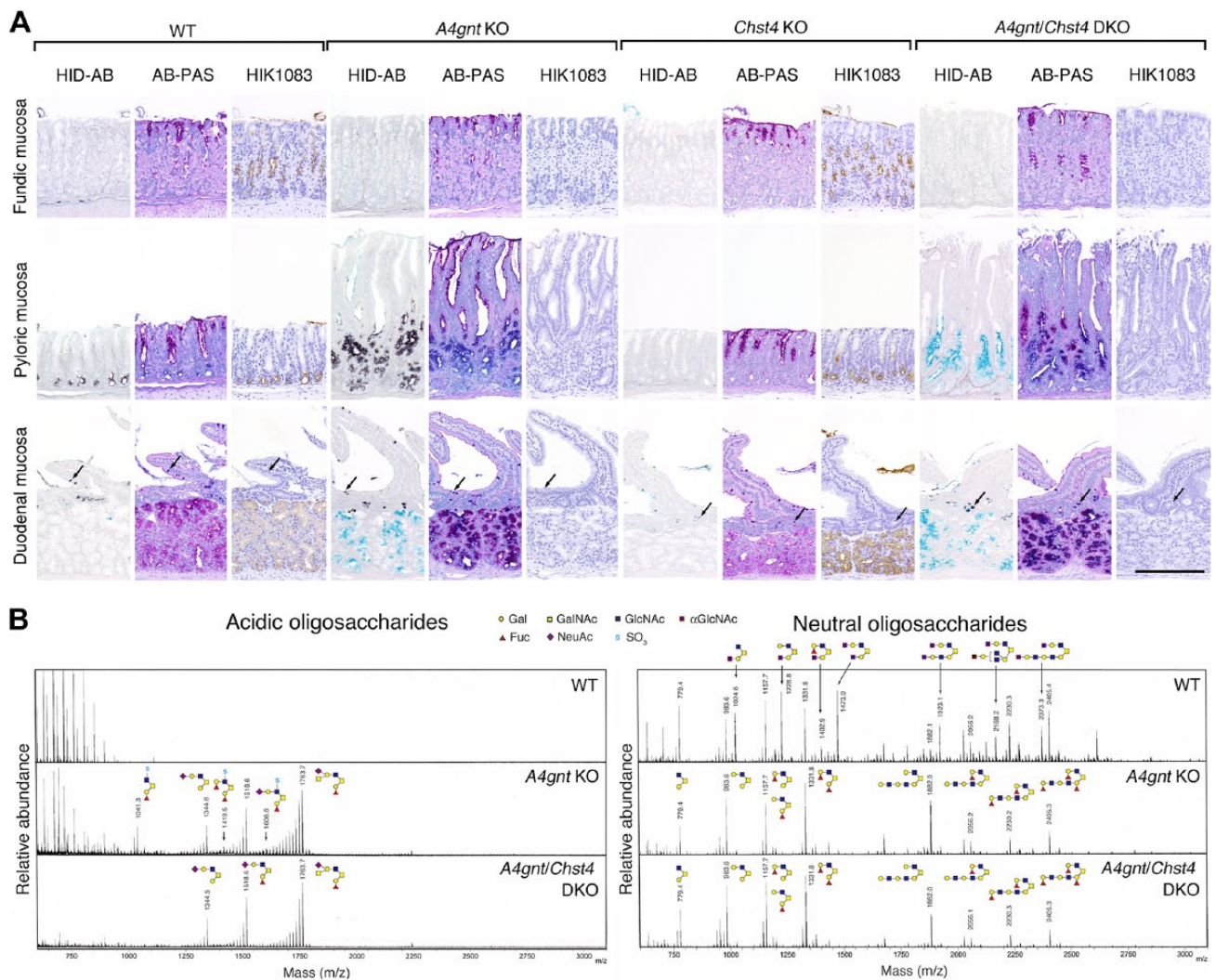


Figure 1. Histochemical, immunohistochemical, and oligosaccharide analyses of sulfomucins and α GlcNAc in gastroduodenal mucosa of 10-week-old mice. (A) HID-AB staining, which differentiates sulfomucins (black color) from sialomucins (sky blue color), AB-PAS staining, which differentiates neutral (red color) from acidic (blue-to-purple color) mucins, and immunohistochemistry using HIK1083 antibody, which is specific for α GlcNAc (HIK1083). Arrows indicate duodenal goblet cells. Bar = 200 μ m. (B) Oligosaccharide analysis of acidic and neutral O-glycans.

three peaks representing sulfated O-glycans in *A4gnt* KO mice were absent in *A4gnt/Chst4* DKO mice. However, sialic acid-containing oligosaccharides were detected in both *A4gnt* KO and *A4gnt/Chst4* DKO mice but not in WT mice. On the other hand, *A4gnt/Chst4* DKO and *A4gnt* KO mice showed comparable levels of neutral oligosaccharides, compare neutral oligosaccharides (right) in *A4gnt* KO versus *A4gnt/Chst4* DKO in Fig. 1B. Overall these results show that GlcNAc6ST-2, which is encoded by the *Chst4* gene, is the sole sulfotransferase responsible for biosynthesis of gastric sulfomucins but not sulfomucins found in duodenal goblet cells. Moreover, given that *A4gnt* KO mice develop gastric cancer,¹² we

conclude that *A4gnt/Chst4* DKO mice are an appropriate mouse model to test effects of sulfomucins on gastric tumorigenesis.

A4gnt/Chst4 DKO Mice Develop Differentiated-type Adenocarcinoma but at a Lower Incidence than do *A4gnt* KO Mice

To assess effects of gastric sulfomucins on gastric tumorigenesis, we examined morphology of gastric mucosa of *A4gnt/Chst4* DKO mice until 60 weeks of age, the same time frame we previously used to examine mucosal morphology in *A4gnt* KO mice.¹² Gross examination of *A4gnt/Chst4* DKO mice revealed the

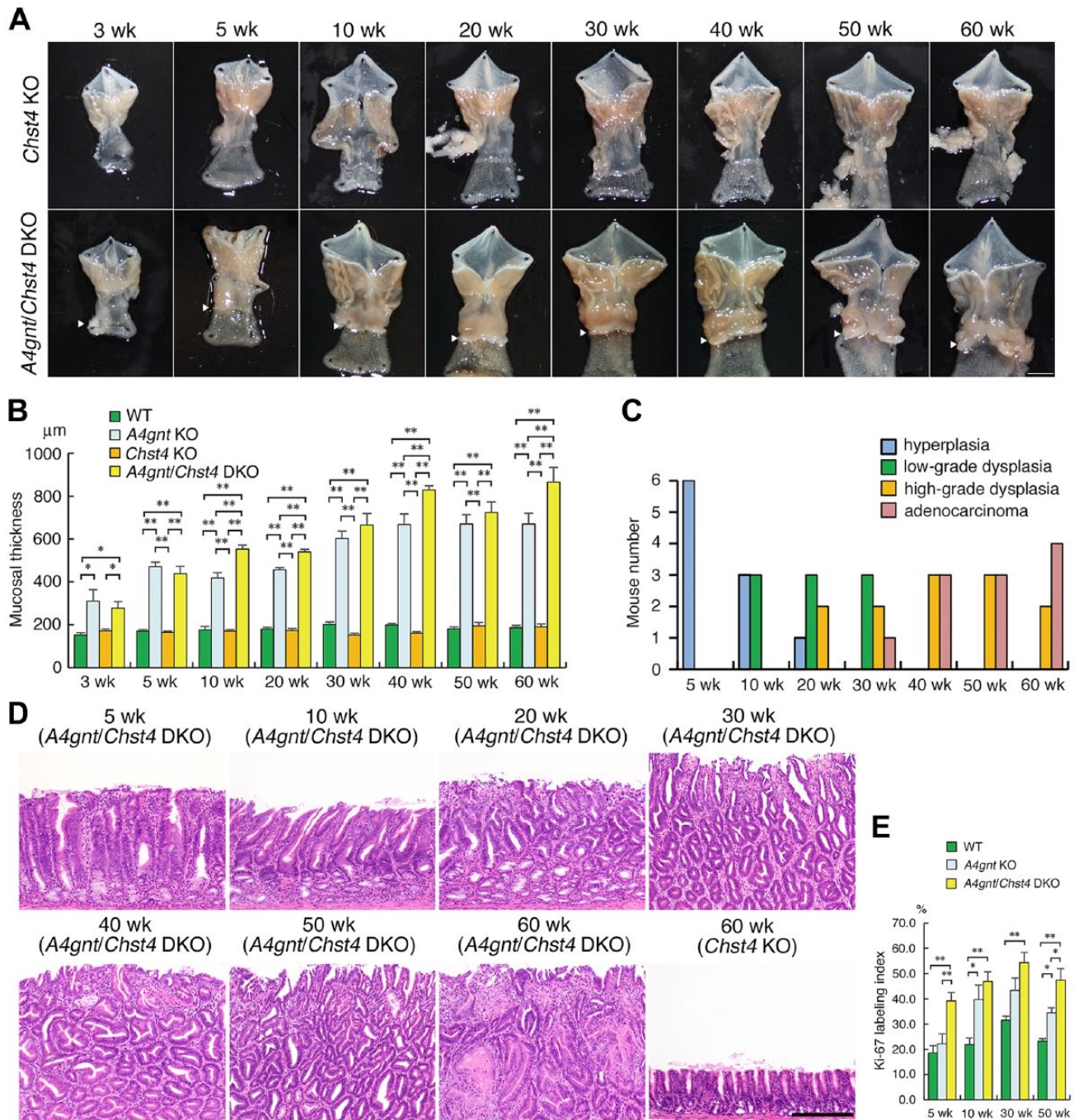


Figure 2. Pathology of mutant mice. (A) Gross appearance of stomach isolated from *Chst4* KO (upper panel) and *A4gnt/Chst4* DKO (lower panel) mice. Arrowheads in DKO samples indicate raised lesions in the pyloric mucosa. Scale bar = 5 mm. wk, weeks. (B) Comparison of pyloric mucosal thickness among WT, *A4gnt* KO, *Chst4* KO, and *A4gnt/Chst4* DKO mice. Each group consists of 6 mice, and data represent the mean \pm SEM. * $P < 0.05$ and ** $P < 0.01$. wk, weeks. (C) Incidence of gastric hyperplasia/dysplasia/adenocarcinoma development in *A4gnt/Chst4* DKO mice during development. Each group consists of 6 mice. wk, weeks. (D) Representative histopathology of the pyloric mucosa from *A4gnt/Chst4* DKO mice. Hyperplasia (at 5 weeks), low-grade dysplasia (at 10 weeks), high-grade dysplasia (at 20–40 weeks), and adenocarcinoma (at 50 and 60 weeks) are shown. Pyloric mucosa of *Chst4* KO mice at 60-weeks-old is shown as a control. Bar = 200 μ m. H&E staining. wk, weeks. (E) Comparison of Ki-67 labeling index in pyloric mucosa in WT, *A4gnt* KO, and *A4gnt/Chst4* DKO mice. Each group consists of 6 mice, and data represent the mean \pm SEM. * $P < 0.05$ and ** $P < 0.01$. wk, weeks.

presence of gastric tumors comparable to those seen in *A4gnt* KO mice¹² appearing in the antrum of the gastric mucosa as mice aged (Fig. 2A). By contrast,

the morphology of the gastric mucosa in *Chst4* KO mice appeared normal. Thickness of the pyloric mucosa of *A4gnt/Chst4* DKO mice was significantly

increased relative to that seen in WT or *Chst4* KO mice at all ages examined (Fig. 2B). Moreover, thickness of the pyloric mucosa of *A4gnt/Chst4* DKO mice was significantly increased relative to that of *A4gnt* KO mice at 10 weeks of age and later, although those differences were less apparent at 30 and 50 weeks of age (Fig. 2B). We observed no significant differences in thickness of gastric mucosa between *Chst4* KO and WT mice at any stage examined.

Histopathological analysis of gastric mucosa from *A4gnt/Chst4* DKO mice showed hyperplasia of the pyloric mucosa ($n = 6/6$) at 5 weeks, low-grade dysplasia ($n = 3/6$) at 10 weeks, and high-grade dysplasia ($n = 2/6$) at 20 weeks (Fig. 2C and D). At 30 weeks of age, adenocarcinoma had developed in 1 of 6 *A4gnt/Chst4* DKO mice, and by 60 weeks of age, at least 50% of *A4gnt/Chst4* DKO mice exhibited differentiated-type adenocarcinoma. Carcinoma cells were limited to the mucosa and did not invade the submucosal layer. Comparable phenotypes reflecting a hyperplasia-dysplasia-adenocarcinoma sequence were seen in *A4gnt* KO mice (supplemental Fig. S3).¹² However, the incidence of gastric cancer development in *A4gnt/Chst4* DKO mice was lower than that seen in *A4gnt* KO mice, as all *A4gnt* KO mice exhibited adenocarcinoma by 50 weeks of age.¹² Finally, like *A4gnt* KO mice,¹² *A4gnt/Chst4* DKO mice showed normal morphology in fundic mucosa of the stomach and duodenal mucosa (data not shown).

We next compared the Ki-67 LI of pyloric epithelial cells at 5-, 10-, 30- and 50-weeks of age among *A4gnt/Chst4* DKO, *A4gnt* KO, and WT mice. The Ki-67 LI of *A4gnt/Chst4* DKO mice was greater than that measured in *A4gnt* KO mice (Fig. 2E): significant differences were seen at 5 ($p < 0.01$) and 50 ($p < 0.05$) weeks. Significant differences in Ki-67 LI were also seen between *A4gnt* KO and WT mice at 10 ($p < 0.05$) and 50 ($p < 0.05$) weeks. These results overall suggest that sulfomucin loss in *A4gnt* KO mice enhances gastric epithelial cell proliferation in pyloric mucosa, but plays a minor role in promoting tumor progression.

A4gnt/Chst4 DKO Mice Spontaneously Develop GCP Emerging through Severe Gastric Erosion

During our analysis of gastric histopathology, we observed that severe gastric erosion accompanied by a marked increase in inflammatory cells occurred in pyloric mucosa of *A4gnt/Chst4* DKO mice at as early as 3 weeks of age ($n = 4/6$) (Fig. 3A). This lesion was seen in almost all of *A4gnt/Chst4* DKO mice examined, irrespective of age ($n = 5/6$ at 5 and 10 weeks of age and $n = 6/6$ at 20–60 weeks of age).

Immunohistochemistry for Ly-6G/Ly-6C (Gr-1) antigen revealed that most of these inflammatory cells were granulocytes (Fig. 3B). By contrast, such severe erosion was not seen in any 3-week-old *A4gnt* KO mice ($n = 0/6$, data not shown). In addition to gastric erosion, GCP, which is defined by the presence of ectopic submucosal glands, subsequently developed beneath the erosion of pyloric mucosa (Fig. 3A). Incidence of GCP at the time points examined was 0/6 at 3 and 5 weeks of age, 2/6 at 10 weeks, 4/6 at 20 weeks, 4/6 at 30 weeks, 3/6 at 40 weeks, 4/6 at 50 weeks, and all 6 mice at 60 weeks.

These results overall indicate that loss of gastric sulfomucins in *A4gnt/Chst4* DKO mice is associated with occurrence of GCP that emerges from severe gastric erosion.

Age-dependent Regulation of Inflammation-related Genes in *A4gnt/Chst4* DKO Mice

We next asked which factors function in the pathogenesis of GCP associated with severe gastric erosion seen in *A4gnt/Chst4* DKO mice. To this end, we investigated expression levels of seven genes encoding the inflammatory chemokines CXCL1, CCL2, and CXCL5, the proinflammatory cytokines IL-1 β and IL-11, and the growth factors HGF and FGF7 by quantitative RT-PCR. All of these factors are reportedly significantly upregulated in *A4gnt* KO relative to WT mice.¹² We also analyzed genes encoding CXCR2,²⁴ CCR2,²⁵ IL1R1/IL1R2,²⁶ IL11RA1,²⁷ MET,²⁸ and FGFR2,²⁹ as they are specific receptors for CXCL1/CXCL5, CCL2, IL-1 β , IL-11, HGF, and FGF7, respectively (Fig. 4).

When *A4gnt/Chst4* DKO mice were 5 weeks of age and showed both severe gastric erosion and hyperplasia, expression levels of *Cxcl1*, *Cxcl5*, *Ccl2*, *Cxcr2*, *Il1b*, and *Il1r2* increased compared to age-matched *A4gnt* KO, *Chst4* KO, and WT mice (Fig. 4, 5 wk). Upregulation of *Il1b* was particularly evident. However, expression of *Il1r1*, which encodes IL1R1, the agonistic IL-1 β receptor, decreased significantly in *A4gnt/Chst4* DKO compared with age-matched *A4gnt* KO and WT mice. In addition, *Il1r2*, which encodes IL1R2, the antagonistic IL-1 β receptor, significantly increased in *A4gnt/Chst4* DKO compared with age-matched *A4gnt* KO, *Chst4* KO, and WT mice, suggesting that the net effects of upregulated IL-1 β may be minimal. Interestingly, expression levels of the six upregulated genes (*Cxcl1*, *Cxcl5*, *Ccl2*, *Cxcr2*, *Il1b*, and *Il1r2*) in *A4gnt/Chst4* DKO mice declined as animals aged, and eventually expression levels of *Cxcl1*, *Cxcr2*, and *Il1r2* in DKO mice showing GCP at 50 weeks of age had significantly decreased relative to those in age-matched *A4gnt* KO mice.

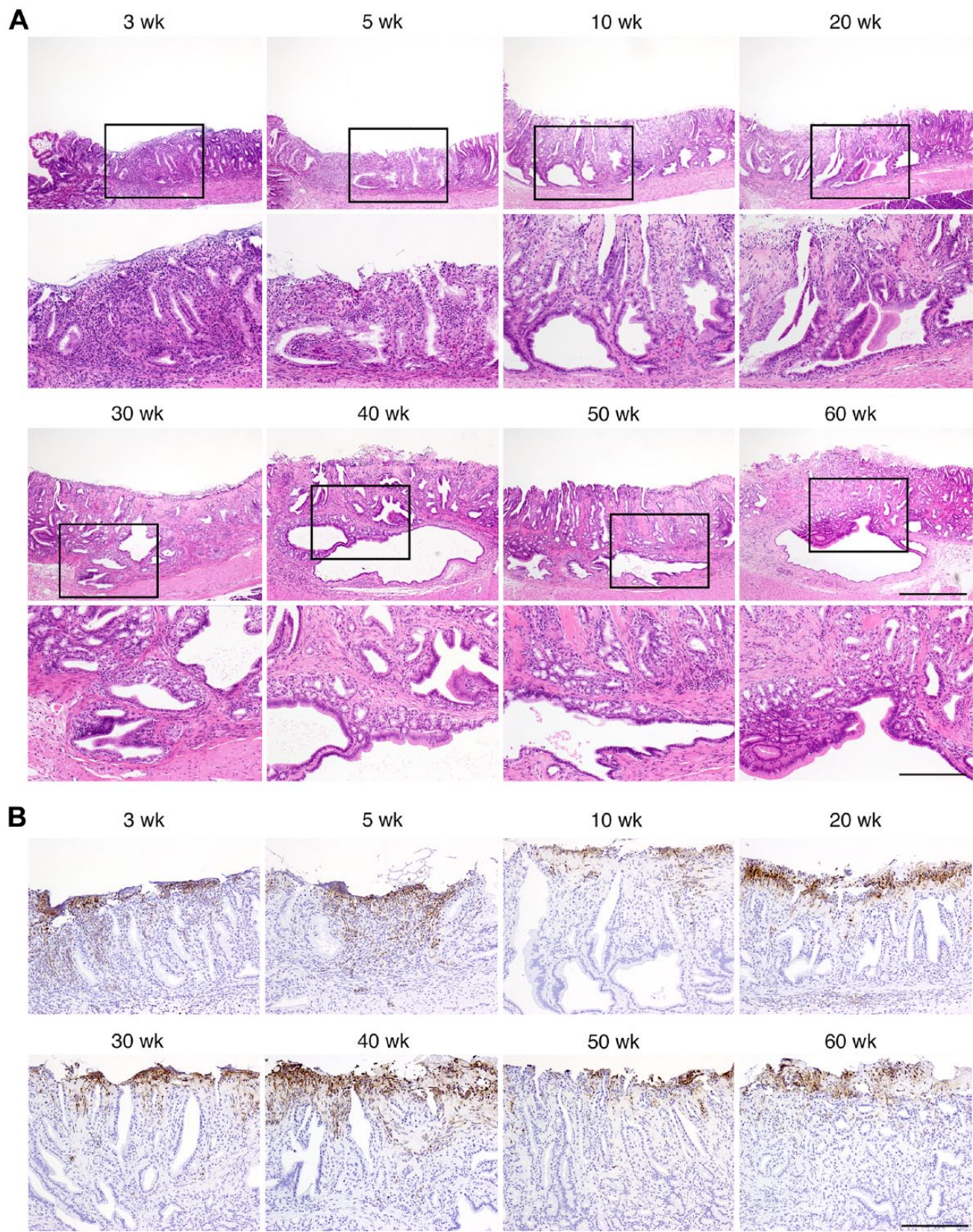


Figure 3. Representative histopathology of severe gastric erosion and GCP in pyloric mucosa of *A4gnt/Chst4* DKO mice. (A) Severe gastric erosion occurred at 3–60 weeks of age, and GCP developed beneath the gastric erosion at 30–60 weeks of age are shown. Lower panels represent higher magnification views of regions boxed in corresponding upper panels. Scale bars in upper and lower panels indicate 500 μ m and 200 μ m, respectively. H&E staining. wk, weeks. (B) Infiltration of granulocytes to severe gastric erosion. Immunohistochemistry for Ly-6G/Ly-6C (Gr-1) antigen. Scale bar indicates 200 μ m. wk, weeks.

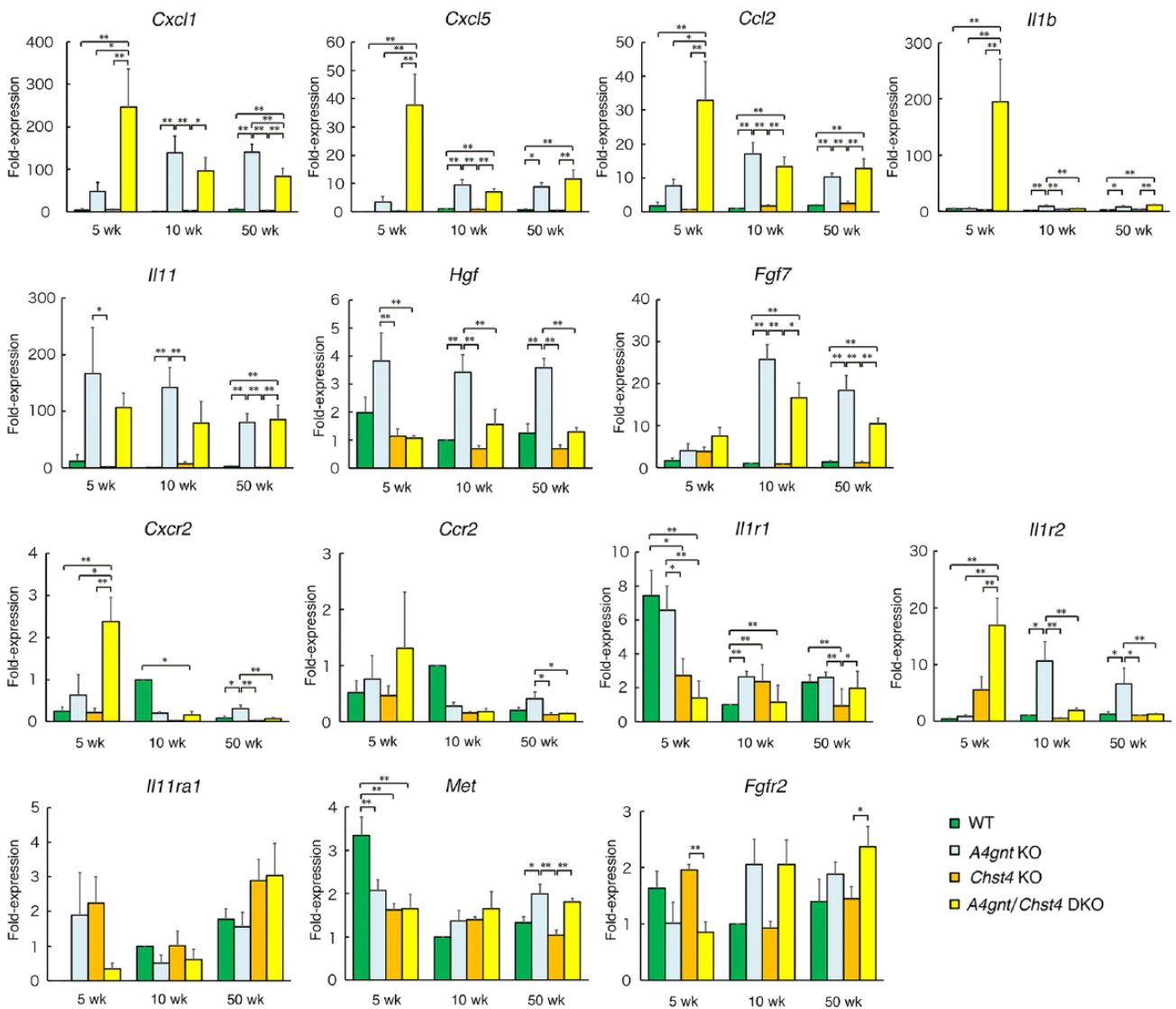


Figure 4. Comparison of expression levels of inflammation-related transcripts at 5, 10, and 50 weeks of age in WT, *A4gnt* KO, *Chst4* KO, and *A4gnt/Chst4* DKO mice, as determined by quantitative RT-PCR. wk, weeks. Fold-expression was calculated relative to the average value seen in 10-week-old WT mice, which was set to 1.0 ($n = 6$). Data derived from other than 10-week-old WT mice represent the mean \pm SEM ($n = 6$ except for 10-week-old *A4gnt/Chst4* DKO mice ($n = 4$), 50-week-old WT mice ($n = 5$), and 50-week-old *A4gnt* KO mice ($n = 5$)). * $P < 0.05$ and ** $P < 0.01$. wk, weeks.

On the other hand, among seven genes (*Cxcl1*, *Ccl2*, *Cxcl5*, *Il1b*, *Il11*, *Hgf*, and *Fgf7*) significantly upregulated in *A4gnt* KO relative to WT mice,¹² expression levels of *Cxcl1*, *Ccl2*, *Il11*, and *Fgf7* were significantly upregulated in 50-week-old *A4gnt* KO and *A4gnt/Chst4* DKO mice showing high-grade dysplasia/adenocarcinoma as compared to age-matched *Chst4* KO and WT mice, which showed normal gastric morphology.

These results suggest that the CXCL1/CXCL5-CCR2 axis, as well as CCL2, functions in severe gastric erosion, while CXCL1, CCL2, IL-11, and FGF7 are associated with gastric carcinogenesis.

Discussion

Here, we first used mucin histochemistry and oligosaccharide analysis to show that GlcNAc6ST-2, which is encoded by *Chst4*, is the sulfotransferase responsible for sulfomucin production in pyloric gland cells of the gastric mucosa of *A4gnt* KO mice. GlcNAc6ST-2 is a carbohydrate sulfotransferase that catalyzes transfer of sulfate from the substrate 3'-phosphoadenosine 5'-phosphosulfate (PAPS) to an *N*-acetylglucosamine residue at the nonreducing terminal of glycans.⁴ It is well known that GlcNAc6ST-2 forms 6-sulfo sialyl

Lewis X on HEV of secondary lymphoid organs or HEV-like vessels appearing in chronic inflammatory tissues in cooperation with GlcNAc6ST-1.^{2,3,6,7} However, deduced oligosaccharide structures of sulfated *O*-glycans detected in *A4gnt* KO mice suggest the presence of Fuc α 1-2Gal β 1-3(SO₃⁻-6GlcNAc β 1-6)GalNAc, Fuc α 1-2Gal β 1-3(Fuc α 1-2Gal β 1-3[SO₃⁻-6]GlcNAc β 1-6)GalNAc, and Fuc α 1-2Gal β 1-3(Neu5Ac α 2-3Gal β 1-3[SO₃⁻-6]GlcNAc β 1-6)GalNAc. Although sulfated residues are attached to GlcNAc of core-2-branched structures in each sulfated *O*-glycan, those residues are distinct from 6-sulfo sialyl Lewis X, which functions as the L-selectin ligand expressed on HEV or HEV-like vessels.^{2,3,6,7} Future study will be of great significance to determine how GlcNAc6ST-2 is induced in the gastric mucosa of *A4gnt* KO mice.

We had initially hypothesized that negatively charged gastric sulfomucins enhance cancer progression by attracting positively charged inflammation-related molecules. To test this hypothesis, we generated *A4gnt/Chst4* DKO mice. Unexpectedly, *A4gnt/Chst4* DKO mice developed differentiated-type gastric adenocarcinoma through a hyperplasia-dysplasia-adenocarcinoma sequence similar to that seen in *A4gnt* KO mice,¹² indicating that gastric sulfomucins play a minor role in gastric tumor progression. Notably, *Cxcl1*, *Ccl2*, *Il11*, and *Fgf7* genes were significantly upregulated in both *A4gnt/Chst4* DKO and *A4gnt* KO mice by 50 weeks of age, and these animals developed high-grade dysplasia/adenocarcinoma not seen in age-matched *Chst4* KO or WT mice, which exhibited normal gastric mucosa. These results suggest a close association of these inflammation-related genes, *Cxcl1*, *Ccl2*, *Il11*, and *Fgf7* with gastric cancer development. Among them, CCL2 and IL-11 are particularly interesting; that is, CCL2 recruits tumor-associated macrophages that promote protumorigenic immune responses.^{30,31} On the other hand, IL-11 is associated with progression of inflammation to gastric tumorigenesis through gp130 signaling, followed by phosphorylation of STAT3.³² Future study is required to determine the signaling mechanism involved in gastric carcinogenesis seen in both *A4gnt* KO and *A4gnt/Chst4* DKO mice.

In the present mucin histochemistry with HID-AB staining, sialomucins in the pyloric mucosa of *A4gnt/Chst4* DKO mice were seemingly much increased compared with those in *A4gnt* KO mice (see Fig. 1A). However, it does not necessarily indicate low amounts of sialomucins in *A4gnt* KO mice. HID-AB staining can barely detect sialomucins simultaneously present with sulfomucins in the same locations, because HID staining is carried out prior to AB staining. Indeed, AB staining alone revealed comparable

amounts of sialomucins in *A4gnt* KO and *A4gnt/Chst4* DKO mice (Supplemental Fig. S4), consistent with the oligosaccharide analysis as shown in Fig. 1B.

Physiological function of gastric sulfomucins seems to be minimal, because no apparent pathological changes were noted in *Chst4* KO mice. However, *Chst4* deletion in *A4gnt* KO mice resulted in severe gastric erosion, followed by GCP. The latter is a rare benign lesion characterized by cystic dilatation of gastric glands extending to the submucosa of the stomach.³³ It is also known that GCP itself is a non-neoplastic lesion but is associated with gastric adenocarcinoma.³⁴ Accordingly, here, GCP seen in *A4gnt/Chst4* DKO mice was associated with adenocarcinoma. Although the pathogenesis is not fully understood, ischemia, chronic inflammation, or foreign bodies present after gastrectomy could be causal factors relevant to GCP.³⁵ KCNE2-KCNQ1 potassium channels are essential for gastric acid secretion from parietal cells of fundic mucosa of the stomach.³⁶ Recently, it was shown that *Kcne2* KO mice develop GCP by 1 year of age.³⁷ The same group demonstrated that these mice exhibit gastric epithelial proliferation of mucous neck cells and chief cells of the fundic mucosa,³⁸ regions that were morphologically normal in *A4gnt/Chst4* DKO mice, indicating that sulfomucin depletion functions in pathogenesis of GCP independent of KCNE2. Our quantitative RT-PCR analysis revealed upregulation of *Cxcl1*, *Cxcl5*, and *Cxcr2* in *A4gnt/Chst4* DKO mice by 5 weeks of age, when severe erosion has developed. On the other hand, *Cxcl1* and *Cxcr2* in *A4gnt/Chst4* DKO mice were downregulated by 50 weeks of age, when GCP had developed, relative to age-matched *A4gnt* KO mice. CXCR2 is a common receptor for CXCL1 and CXCL5, and the *Cxcl1/Cxcl5-Cxcr2* axis is associated with neutrophil infiltration.³⁹ Thus, it is likely that granulocytes markedly infiltrating to severe erosion in *A4gnt/Chst4* DKO mice could be recruited by the *Cxcl1/Cxcl5-Cxcr2* axis, and such an inflammatory response may trigger erosion, eventually resulting in GCP. It will be of great interest to determine the molecular mechanism including signaling pathways how gastric sulfomucins maintain mucosal integrity by analyzing *A4gnt/Chst4* DKO mice.

In conclusion, gastric sulfomucins formed by the sulfotransferase GlcNAc6ST-2 are overproduced in *A4gnt* KO mice, which spontaneously develop differentiated-type adenocarcinoma of the stomach. By analyzing *A4gnt/Chst4* DKO mice, we established that gastric sulfomucins protect the gastric mucosa from developing GCP emerging from gastric erosion but play a minor role in development of gastric carcinogenesis.

Acknowledgment

The authors thank Dr. Elise Lamar for editing the manuscript.

Competing Interests

The author(s) declared no potential conflicts of interest with respect to the research, authorship, and/or publication of this article.

Author Contributions

MK, MNF, MF, and JN conceived and designed research; MK, HKo, YG, MO, YS, CF, MM, NA, SH, KY, SY, and JN performed experiments and analyzed data; MK, HKo, YG, SK, HKa, MNF, MF, and JN interpreted results of experiments; MK, HKo, YG, and JN drafted the manuscript. All authors have read and approved the final manuscript.

Funding

The author(s) disclosed receipt of the following financial support for the research, authorship, and/or publication of this article: This study was supported by Grants-in-Aid for Scientific Research from the Japan Society for the Promotion of Science, nos. 16K08708 (MK), 17K17779 (HKo), and 15H04712 (JN).

Literature Cited

- Nieuw Amerongen AV, Bolscher JG, Bloemena E, Veerman EC. Sulfomucins in the human body. *Biol Chem*. 1998;379:1–18.
- Kawashima H. Roles of sulfated glycans in lymphocyte homing. *Biol Pharm Bull*. 2006;29:2343–9.
- Kobayashi M, Hoshino H, Suzawa K, Sakai Y, Nakayama J, Fukuda M. Two distinct lymphocyte homing systems involved in the pathogenesis of chronic inflammatory gastrointestinal diseases. *Semin Immunopathol*. 2012;34:401–13.
- Hiraoka N, Petryniak B, Nakayama J, Tsuboi S, Suzuki M, Yeh JC, Izawa D, Tanaka T, Miyasaka M, Lowe JB, Fukuda M. A novel, high endothelial venule-specific sulfotransferase expresses 6-sulfo sialyl Lewis(x), an L-selectin ligand displayed by CD34. *Immunity*. 1999;11:79–89.
- Yeh J-C, Hiraoka N, Petryniak B, Nakayama J, Ellies LG, Rabuka D, Hindsgaul O, Marth JD, Lowe JB, Fukuda M. Novel sulfated lymphocyte homing receptors and their control by a core1 extension β 1,3-N-acetylglucosaminyltransferase. *Cell*. 2001;105:957–69.
- Kawashima H, Petryniak B, Hiraoka N, Mitoma J, Huckaby V, Nakayama J, Uchimura K, Kadomatsu K, Muramatsu T, Lowe JB, Fukuda M. N-acetylglucosamine-6-O-sulfotransferase-1 and -2 cooperatively control lymphocyte homing through L-selectin ligand biosynthesis in high endothelial venules. *Nat Immunol*. 2005;6:1096–104.
- Uchimura K, Gauguier JM, Singer MS, Tsay D, Kannagi R, Muramatsu T, von Andrian UH, Rosen SD. A major class of L-selectin ligands is eliminated in mice deficient in two sulfotransferases expressed in high endothelial venules. *Nat Immunol*. 2005;6:1105–13.
- Kobayashi M, Mitoma J, Nakamura N, Katsuyama T, Nakayama J, Fukuda M. Induction of peripheral lymph node addressin in human gastric mucosa infected by *Helicobacter pylori*. *Proc Natl Acad Sci USA*. 2004;101:17807–12.
- Suzawa K, Kobayashi M, Sakai Y, Hoshino H, Watanabe M, Harada O, Ohtani H, Fukuda M, Nakayama J. Preferential induction of peripheral lymph node addressin on high endothelial venule-like vessels in the active phase of ulcerative colitis. *Am J Gastroenterol*. 2007;102:1499–509.
- Gad A. A histochemical study of human alimentary tract mucosubstances in health and disease. I. Normal and tumours. *Br J Cancer*. 1969;23:52–63.
- Yamanoi K, Nakayama J. Reduced α GlcNAc glycosylation on gastric gland mucin is a biomarker of malignant potential for gastric cancer, Barrett's adenocarcinoma, and pancreatic cancer. *Histochem Cell Biol*. 2018;149:569–75.
- Karasawa F, Shiota A, Goso Y, Kobayashi M, Sato Y, Masumoto J, Fujiwara M, Yokosawa S, Muraki T, Miyagawa S, Ueda M, Fukuda MN, Fukuda M, Ishihara K, Nakayama J. Essential role of gastric gland mucin in preventing gastric cancer in mice. *J Clin Invest*. 2012;122:923–34.
- Spicer SS. Diamine methods for differentiating mucosubstances histochemistry. *J Histochem Cytochem*. 1965;13:211–234.
- Hiraoka N, Kawashima H, Petryniak B, Nakayama J, Mitoma J, Marth JD, Lowe JB, Fukuda M. Core 2 branching β 1,6-N-acetylglucosaminyltransferase and high endothelial venule-restricted sulfotransferase collaboratively control lymphocyte homing. *J Biol Chem*. 2004;279:3058–67.
- Avey MT, Fenwick N, Griffin G. The use of systematic reviews and reporting guidelines to advance the implementation of the 3Rs. *J Am Assoc Lab Anim Sci*. 2015;54:153–62.
- Fenoglio-Preiser C, Muñoz N, Carneiro F, Powell SM, Correa P, Rugge M, Guilford P, Sasako M, Lambert R, Stolte M, Megraud F, Watanabe H. Gastric carcinoma. In: Hamilton SR, Aaltonen LA, editors. *Pathology and genetics of tumours of the digestive system*. Lyon: IARC Press; 2000. p. 39–52.
- Akiyama S, Mochizuki W, Nibe Y, Matsumoto Y, Sakamoto K, Oshima S, Watanabe M, Nakamura T. CCN3 expression marks a sulfomucin-nonproducing unique subset of colonic goblet cells in mice. *Acta Histochem Cytochem*. 2017;50:159–68.
- Ishihara K, Kurihara M, Goso Y, Urata T, Ota H, Katsuyama T, Hotta K. Peripheral α -linked N-acetylglucosamine on the carbohydrate moiety of mucin derived from mammalian gastric gland mucous cells: epitope recognized by a newly characterized monoclonal antibody. *Biochem J*. 1996;318(Pt 2):409–16.
- Benson MJ, Elgueta R, Schpero W, Molloy M, Zhang W, Usherwood E, Noelle RJ. Distinction of the memory

- B cell response to cognate antigen versus bystander inflammatory signals. *J Exp Med*. 2009;206:2013–25.
20. Fleming TJ, Fleming ML, Malek TR. Selective expression of Ly-6G on myeloid lineage cells in mouse bone marrow. RB6-8C5 mAb to granulocyte-differentiation antigen (Gr-1) detects members of the Ly-6 family. *J Immunol*. 1993;151:2399–408.
 21. Ciucanu I, Costello CE. Elimination of oxidative degradation during the per-O-methylation of carbohydrates. *J Am Chem Soc*. 2003;125:16213–9.
 22. Khoo KH, Yu SY. Mass spectrometric analysis of sulfated N- and O-glycans. *Methods Enzymol*. 2010;478:3–26.
 23. Ceroni A, Maass K, Geyer H, Geyer R, Dell A, Haslam SM. GlycoWorkbench: a tool for the computer-assisted annotation of mass spectra of glycans. *J Proteome Res*. 2008;7:1650–9.
 24. Verbeke H, Geboes K, Van Damme J, Struyf S. The role of CXC chemokines in the transition of chronic inflammation to esophageal and gastric cancer. *Biochim Biophys Acta*. 2012;1825:117–29.
 25. Lim SY, Yuzhalin AE, Gordon-Weeks AN, Muschel RJ. Targeting the CCL2-CCR2 signaling axis in cancer metastasis. *Oncotarget*. 2016;7:28697–710.
 26. Stylianou E, Saklatvala J. Interleukin-1. *Int J Biochem Cell Biol*. 1998;30:1075–9.
 27. Putoczki T, Ernst M. More than a sidekick: the IL-6 family cytokine IL-11 links inflammation to cancer. *J Leukoc Biol*. 2010;88:1109–17.
 28. Matsumoto K, Umitsu M, De Silva DM, Roy A, Bottaro DP. Hepatocyte growth factor/MET in cancer progression and biomarker discovery. *Cancer Sci*. 2017;108:296–307.
 29. Grose R, Dickson C. Fibroblast growth factor signaling in tumorigenesis. *Cytokine Growth Factor Rev*. 2005;16:179–86.
 30. Mantovani A, Allavena P, Sica A, Balkwill F. Cancer-related inflammation. *Nature*. 2008;454:436–44.
 31. Grivennikov SI, Greten FR, Karin M. Immunity, inflammation, and cancer. *Cell*. 2010;140:883–99.
 32. Howlett M, Giraud AS, Lescesen H, Jackson CB, Kalantzis A, Van Driel IR, Robb L, Van der Hoek M, Ernst M, Minamoto T, Boussioutas A, Oshima H, Oshima M, Judd LM. The interleukin-6 family cytokine interleukin-11 regulates homeostatic epithelial cell turnover and promotes gastric tumor development. *Gastroenterology*. 2009;136:967–77.
 33. Franzin G, Novelli P. Gastritis cystica profunda. *Histopathology*. 1981;5:535–47.
 34. Mitomi H, Iwabuchi K, Amemiya A, Kaneda G, Adachi K, Asao T. Immunohistochemical analysis of a case of gastritis cystica profunda associated with carcinoma development. *Scand J Gastroenterol*. 1998;33:1226–9.
 35. Fonde EC, Rodning CB. Gastritis cystica profunda. *Am J Gastroenterol*. 1986;81:459–64.
 36. Heitzmann D, Grahammer F, von Hahn T, Schmitt-Gräff A, Romeo E, Nitschke R, Gerlach U, Lang HJ, Verrey F, Barhanin J, Warth R. Heteromeric KCNE2/KCNQ1 potassium channels in the luminal membrane of gastric parietal cells. *J Physiol*. 2004;561(Pt 2):547–57.
 37. Roepke TK, Purtell K, King EC, La Perle KM, Lerner DJ, Abbott GW. Targeted deletion of *Kcne2* causes gastritis cystica profunda and gastric neoplasia. *PLoS ONE*. 2010;5:e11451.
 38. Roepke TK, Anantharam A, Kirchhoff P, Busque SM, Young JB, Geibel JP, Lerner DJ, Abbott GW. The KCNE2 potassium channel ancillary subunit is essential for gastric acid secretion. *J Biol Chem*. 2006;281:23740–7.
 39. Jablonska J, Wu CF, Andzinski L, Leschner S, Weiss S. CXCR2-mediated tumor-associated neutrophil recruitment is regulated by IFN- β . *Int J Cancer*. 2014;134:1346–58.